Geologie en Mijnbouw 67: 313–332 (1988)


# Stratiform Zn-Pb-Fe-Mn mineralization in the Älvlången-Vikern area, Bergslagen, Sweden

Rob H. Hellingwerf[1], Robert Lilljequist[2] & Sigvard Ljung[3]
[1] *Geologisch Museum, Nieuwe Prinsengracht 130, 1018 VZ Amsterdam, The Netherlands; present address: Instituut voor Aardwetenschappen, Rijks Universiteit Utrecht, P.O. Box 80.021, 3508 TA Utrecht, The Netherlands;*
[2] *Swedish Geological AB, Box 1424, S-751 44 Uppsala, Sweden;*
[3] *State Mining Property Commission, S-117 80 Stockholm, Sweden*

Received 1 July 1987; accepted in revised form 23 November 1987

*Key words:* stratiform, lead-zinc, tourmaline, exhalites, Bergslagen, Sweden

**Abstract**

The stratiform Zn-Pb sulphide mineralization of the Älvlången-Vikern area, central Sweden, is contained in an iron-rich meta-sedimentary unit at the base of a sequence of dolomitic marble and metachert of Mid-Proterozoic age, deposited in a fault-bounded sedimentary basin. This basin probably developed during a phase of extensional tectonics. The mineralized unit is a steeply south-easterly dipping zone of 6 km long, extending from Lake Vikern in the NE to Lake Älvlången in the SW. Sphalerite, galena, magnetite and minor arsenopyrite, pyrite, pyrrhotite, chalcopyrite and marcasite occur in fine-grained, well banded and laminated garnet-biotite-cummingtonite-tourmaline-rich rocks of presumably sedimentary-exhalative origin. Characteristic are the small quantities of scapolite and orthite, and the high Ba and C1 contents of various micas and amphiboles. Apart from Zn, Pb, Fe, Mn, Ba and C1 the ore zone is enriched in As, Sb, Ag, Ba, Th, U, Ti, Cr, Co, Ni and V. A distinct metal (Zn + Pb → Fe + Mn + Ba) and mineral (sulphides + tourmaline → oxides + cummingtonite) zonation has been observed along the ore zone from the centre, where Zn and Pb contents are highest, to the margin of the basin.

The marbles just below the ore zone are locally brecciated, showing network veins with phlogopite, tourmaline and traces of chalcopyrite and pyrrhotite, and corroded rhyolitic fragments. This brecciation of marbles is associated with extreme calc-silicate alteration of intercalated metatuffites and metacherts along veins and fractures. The breccias and calc-silicate alteration, occurring in narrow zones following the fault-bounded basin, are considered to represent hydrothermal feeder channels.

The metapyroclastic rocks below the ore-hosting marbles are albitized, microclinized, sericitized, biotitized, calc-silicate altered, silicified, and tourmalinized. Of these, the first three are regional alteration types, presumably not significantly related to the ore-forming processes, whereas the latter four are localized, ore-related alteration types, occurring mostly along network veins and fractures.

Tourmaline is a characteristic, but minor, constituent of all rock types below and within the ore zone. The highest concentrations occur in and below the central part of the basin, where the highest sulphide contents occur. It is absent in rocks overlying the ore zone, suggesting tourmaline to be a mineralogical exploration guide.

Circulation of the hydrothermal fluids is thought to have initiated during rifting and driven by a high geothermal gradient beneath the depression. This high geothermal gradient may partially be attributed to a hidden felsic magma plug below the ore zone, as indicated by the rhyolitic fragments in the hydrothermal marble breccias.

## Introduction

Volcanogenic and sediment-hosted stratiform orebodies of Lower to Middle Proterozoic age are among the world's largest resources of zinc, lead, copper, cadmium, silver and gold (Sangster, 1976; Stanton, 1986). They occur as lenses and more blanket-like deposits parallel to the layering of the volcano-sedimentary host rocks, and consist of varying concentrations of sphalerite, galena, pyrite, chalcopyrite and pyrrhotite. Apart from the usual rock-forming silicates and carbonates, fluorite, barite and/or tourmaline are associated with the sulphides (Sangster & Scott, 1976; Plimer, 1979, 1986; Slack, 1982; Stanton, 1986). The underlying rocks may contain discordant feeder zones that are silicified, chloritized, sericitized, or tourmalinized (e.g. Sangster & Scott, 1976). The majority of such stratiform deposits tends to occur in areas of extensional tectonics near fault zones and near volcanic centres (Russell et al., 1981; Plimer, 1986; Sawkins, 1986; Stanton, 1986). The Mid-Proterozoic zinc-lead mineralization of the Älvlången-Vikern area in central Sweden is hosted by a sequence of volcano-sedimentary rocks belonging to the Bergslagen Supracrustal series, which is also considered to have formed in an extensional environment (Oen et al., 1982; Van der Velden et al., 1982; Helmers, 1984; Vivallo & Rickard, 1984; Baker, 1985; Hellingwerf & Oen, 1986; Hellingwerf, 1986; Oen, 1987).

The Älvlången-Vikern area is an old mining area, described as 'Vikersfältet', with a number of banded iron oxide deposits that are locally more sulphide-rich (Santesson, 1889; Geijer & Magnusson, 1944). From 1857–1902 iron ore was produced in a number of small, NE-SW aligned excavations in the sulphide-poor, Ca-Mg-Mn-rich parts of the mineralization. The iron ore occurred at several levels, with thicknesses less than 10 m, though a repetition of layers due to isoclinal folding was suspected (Santesson, 1889). Hydrothermal alteration in the underlying rocks may have a genetic relationship with the mineralization. Recently, the State Mining Property Commission and Swedish Geological AB started a Zn-Pb sulphide prospection program in the area, the results of which form the basis of the present study. This paper reports on 1) the relationship between the stratiform Zn-Pb-Fe-Mn mineralization and the hydrothermal alteration in the underlying rocks, 2) the lateral metal and mineral zonations, 3) the reconstruction of the sedimentary basin, and 4) the use of tourmaline and whole-rock geochemistry as prospection tools.

## Samples and applied techniques

Samples were collected from surface exposures and small excavations. Polished thin sections were examined by standard transmitted and reflected light microscopy. Whole-rock major and trace elements (Table 1) were analyzed at the laboratories of Sveriges Geologiska AB in Luleå, Sweden, using I.C.P. techniques with total dissolution in HF/ $HC10_4$.

## Regional stratigraphy and geological setting

The Zn-Pb-mineralized marble-metachert sequence of Älvlången-Vikern is underlain by a thick pile of felsic metapyroclastic rocks with quartz-banded iron oxide ores, and overlain by a pile of well-banded metatuffites of presumably mixed tuffaceous and chemical origin. This metavolcanite-marble-metatuffite sequence is thought to be equivalent to the Middle Leptite group and Upper Leptite-hälleflinta and Slate group as described by Oen et al. (1982) for the Filipstad-Grythyttan-Hjulsjö area, roughly 40 km NE of Älvlången-Vikern. The latter volcano-sedimentary sequence is a 1.9 to 1.8 Ga old chronostratigraphic unit (Welin et al., 1980; Oen et al., 1982), previously interpreted to have formed above a subduction zone (Hietanen, 1975; Löfgren, 1979; Loberg, 1980). However, Oen et al. (1982) suggested that the sequence was deposited in a rifting environment, supported by the bimodal nature of the felsic and mafic volcanic rocks (Van der Velden et al., 1982). Later support came from the paleogeographic orientation of the sedimentary basins (Helmers, 1984), the geochemistry of anorogenic granitic intrusions (Baker, 1985), the style of granite-hosted disseminated molybdenum occurrences (Hellingwerf & Baker, 1985), and the continental tholeiitic composition of the least altered mafic rocks (Hellingwerf & Oen, 1986). Similar extensional environments have also been suggested for other areas in Bergslagen (e.g. Vivallo & Rickard, 1984). A phase of regional compressive deformation, subsequent to the extensional tectonics, occurred at about 1.84 Ga (Oen et al., 1982), and contributed to the overall steep orientation of the strata.

## Local geology

The stratigraphically lowermost rocks of the Älvlången-Vikern area consist of felsic metavolcanites with quartz-banded iron oxide ores and a few sheet-like metabasic intrusions (Fig. 1). The metavolcanites are quartz- and feldspar phenocryst-rich pyroclastic rocks, occasionally containing rock fragments. On top of these rocks a sequence of marble with metachert intercalations is deposited

*Table 1.* Two selected and five average chemical analyses of Älvlången-Vikern rock types.

| | 1 (n=1) | 2 (n=1) | 3 (n=7) | 4 (n=3) | 5 (n=7) | 6 (n=7) | 7 (n=2) |
|---|---|---|---|---|---|---|---|
| (wt %) | | | | | | | |
| $TiO_2$ | 0.17 | 0.16 | 0.20 | 0.78 | 0.22 | 0.17 | 0.32 |
| $Al_2O_3$ | 10.7 | 10.5 | 10.7 | 12.9 | 9.6 | 6.7 | 11.6 |
| $Fe_2O_3$ | 2.1 | 1.8 | 3.2 | 7.8 | 13.7 | 28.0 | 4.6 |
| MnO | 0.01 | 0.01 | 0.05 | 0.10 | 1.21 | 2.17 | 0.23 |
| MgO | 1.1 | 2.5 | 2.2 | 3.3 | 3.5 | 5.3 | 9.7 |
| CaO | 0.8 | 0.3 | 1.0 | 2.0 | 2.3 | 2.0 | 10.9 |
| $Na_2O$ | 4.30 | 2.20 | 0.40 | 2.59 | 0.15 | 0.12 | 0.19 |
| $K_2O$ | 1.1 | 2.7 | 5.4 | 3.2 | 3.3 | 2.1 | 2.8 |
| $P_2O_5$ | 0.02 | 0.02 | 0.02 | 0.18 | 0.11 | 0.08 | 0.09 |
| (ppm) | | | | | | | |
| Sc | 5 | 5 | 3 | 21 | 5 | 3 | 7 |
| Cr | 2 | 1 | 4 | 8 | 13 | 12 | 15 |
| Co | – | – | 3 | 14 | 11 | 38 | 19 |
| Ni | 5 | 5 | 10 | 9 | 11 | 9 | 12 |
| Cu | 10 | 9 | 13 | 11 | 33 | 87 | 24 |
| Zn | 6 | 3 | 26 | 154 | 14476 | 6142 | 18275 |
| Rb | 53 | 87 | 110 | 72 | 113 | 88 | 93 |
| Sr | 110 | 25 | 11 | 51 | 10 | 11 | 24 |
| Y | 20 | 13 | 31 | 27 | 33 | 26 | 25 |
| Zr | 200 | 190 | 241 | 160 | 154 | 118 | 180 |
| Sb | – | – | 15 | 7 | 16 | 20 | 97 |
| Ba | 280 | 320 | 1534 | 503 | 658 | 2539 | 240 |
| Pb | 8 | 8 | 15 | 41 | 1787 | 2853 | 43085 |
| Th | 9 | 19 | 19 | 10 | 20 | 17 | 7 |
| U | 21 | 22 | 21 | – | 39 | 124 | 27 |
| La | 31 | 64 | 29 | 20 | 46 | 33 | 51 |
| Ag | 1 | 2 | 2 | 2 | 12 | 19 | 91 |
| Li | – | 2 | 33 | 14 | 36 | 24 | 40 |
| Cd | – | – | – | – | 40 | 34 | 45 |
| V | 1 | – | 9 | 88 | 22 | 25 | 32 |

1 Albitized metavolcanite, N of Kopparskallen
2 K-altered metavolcanite, same locality as 1
3 Regionally K-enriched metavolcanites
4 Locally altered, biotitized metavolcanites
5 Central garnet-biotite-rich ores
6 Peripheral garnet-biotite-cummingtonite-rich ores
7 Sulphide-disseminated quartz-mica-rich metacherts

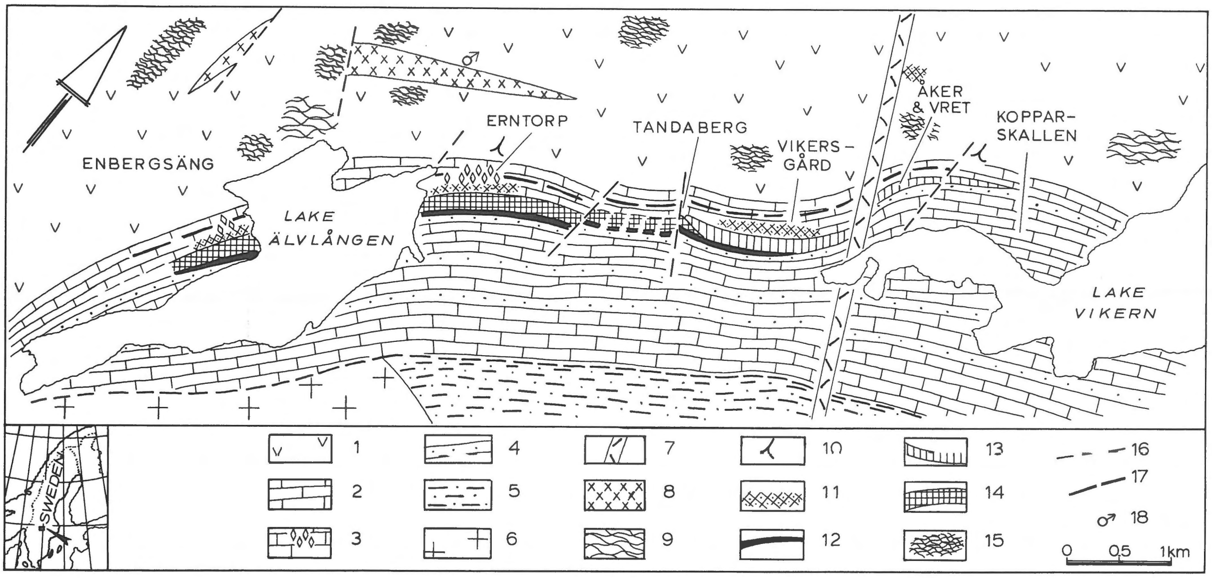


*Fig. 1.* Simplified geological map of the Älvlången-Vikern area. 1 – felsic metavolcanite; 2 – marble; 3 – marble breccia; 4 – metatuffite and metachert intercalations; 5 – metatuffite; 6 – Filipstad-type granite; 7 – dolerite dyke; 8 – metabasite; 9 – silicification; 10 – quartz-tourmaline veins; 11 – calc-silicate alteration; 12 – areal distribution of Zn-Pb sulphides; 13 – garnet-biotite-cummingtonite-rich rock; 14 – garnet-biotite-rich rock; 15 – biotitization; 16 – minor fault; 17 – major fault; 18 – banded iron oxide ore. The younging direction is from N to S.

in a NE-SW trending basin, hosting the Zn-Pb-bearing iron ore horizon. This horizon becomes more sulphide-rich along strike towards the SW. North of this sulphide-rich zone, at lower stratigraphic levels, marble breccias, rich in phlogopite and tourmaline, and calc-silicate-altered metacherts and metavolcanites occur in zones of roughly 100 m wide and several hundreds of meters long. They are aligned parallel to the sulphide-rich zone, and are oriented along the NE-SW trending fault zone that borders the sedimentary basin to the N.

The whole marble – sulphide-zone – metachert sequence is in contact with, and possibly overlain by a pile of well-banded and laminated calc-silicate-rich, banded metatuffites. The contact between the marbles and metatuffites is largely tectonic; a NE-SW striking fault zone borders the marbles to the S. This fault zone runs roughly parallel to the general strike of the basin, and also parallel to the fault zone that borders the basin to the N (Fig. 1). A Filipstad-type granite, that intruded the sequence after a phase of compressive deformation, is also affected in this southern fault zone. From field observations it is not clear whether the southern fault zone is from the same age as the northern fault zone, making the basin an entirely fault-bounded graben, and re-activated after intrusion of the granite, or from a younger age, unrelated to the northern fault zone, making the basin a half graben.

The phase of regional compressive deformation, subsequent to the extensional tectonics during which the basin developed, caused the steep orientation of the entire volcano-sedimentary sequence. The latest magmatic activity is represented by thin dolerite dykes that intruded the area in NNW direction (Fig. 1).

## Configuration, mineral assemblages and textures of the zinc-lead horizon

### *General features*

The stratiform Älvlången-Vikern zinc-lead horizon can be classified as an 'Åmmeberg-type' deposit among the Swedish zinc-lead deposits (Mag-

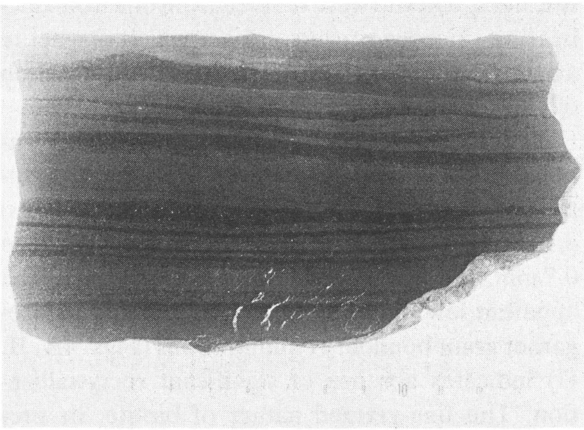

*Fig. 2.* Finely laminated garnet-biotite-sphalerite-magnetite sample from Erntorp. Length of specimen is appr. 15 cm.

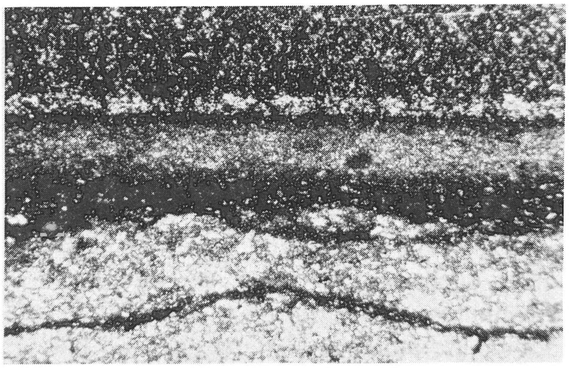

*Fig. 3.* Microphotograph of phlogopite-tourmaline layers (black and grey) in marble (white). Between Vikersgård and Åkergruvan, plane polarized light. Field of view is 3 × 2 mm.

nusson, 1950). It extends 3 km from Lake Vikern in the NE to Lake Älvlången in the SW (Fig. 1), and dips steeply towards the SE. On the basis of geophysical data, the zone continues under Lake Älvlången in SW direction. The sulphides are associated with a manganiferous iron-rich horizon, hosted by a sequence of marble, metachert and minor jasperoid rocks. The zinc-lead horizon mimics the layered, laterally-continuous nature of the host rock meta-sediments and can be classified as a transitional type between pure volcanogenic and pure sediment-hosted sulphide deposits, on the basis of 1) the blanket-like morphology with lateral extents up to 6 km, hundreds of times greater than its thickness; 2) the relative Zn-Pb-rich -, Cu-poor nature of the mineralization, typical for sedimentary environments (Sangster & Scott, 1976; Sangster, 1986); 3) its stratigraphic position just above the main volcanic pile; and 4) the mixed volcano-sedimentary sequence of the host rocks. According to Sangster & Scott (1976) such deposits are the next most common sulphide deposits after the pure volcanogenic deposits.

The mineralized zone itself consists of sulphide- and magnetite-rich layers occurring in well-banded and laminated garnet-biotite-cummingtonite-tourmaline-rich rocks with minor Ba-Cl-rich micas, orthite and scapolite. Sphalerite and galena, making up the bulk of the sulphide horizon, occur in two different ways: 1) as aggregates and intergrowths with garnet in well banded and laminated garnet-biotite-rich rocks, showing metal contents up to 3.8% Zn, 1.1% Pb, 37.9% Fe, 3.6% Mn and 42 ppm Ag, and 2) as fine-grained, dusty disseminations in calc-silicate-free quartz-biotite-rich metachert layers with up to 2.4% Zn, 6.9% Pb, 6.9% Fe, .2% Mn and 110 ppm Ag.

The garnet-biotite-rich rocks are, volumetrically, the dominant sulphide-hosting rocks of the ore zone. They show a ubiquitous fine-scale mineralogical layering, that undoubtedly represents original bedding (Figs. 2 & 3), expressed by varying proportions of garnet, biotite, cummingtonite, tourmaline, magnetite and sulphides in .5 mm to 40 cm thick bands intercalated in marble. Within these silicate-rich bands, thin, 1 to 10 mm thick, garnet-rich layers alternate with biotite-rich and/or cummingtonite-rich layers. Occasionally, 5 mm thick monomineralic garnet layers occur without any evidence for single crystals. Locally, layering is expressed by changes in grain sizes.

The galena-sphalerite-dusted metachert layers are homogeneous, fine-grained quartz-biotite-rich rocks, with little banding, and a clear foliation parallel to the regional NE-SW direction. This type of mineralization is of minor importance and has only been found NE and W of Lake Älvlången.

In both types of mineralization, calcite-sphalerite-galena-chlorite-magnetite-arsenopyrite veins traverse the ore samples. Especially in the quartz-biotite-rich metacherts they occur at high and low angles with the foliation. These veins are not regarded as a second phase of mineralization, but as mobilization features during soft rock hydrothermal metamorphism (Oen & Hellingwerf, 1988, this issue).

*Mineral textures*

*Garnet* occurs as isolated, massive poikiloblasts and as zoned porphyroblastic aggregates in biotite- or cummingtonite-rich layers (Figs. 4A-4D), and as continuous, monomineralic layers of a few mm thick. The zoned garnets show a massive, occasionally pinkish core and a colourless rim with abundant inclusions. Preliminary electron microprobe analyses (Table 2) indicate almandine-rich compositions with a minor spessartite component showing 'normal' (Mn-enriched, Fe-depleted core relative to the rim) and 'reverse' (Mn-depleted, Fe-enriched core relative to the rim) zonations (Hellingwerf et al. in prep.). Grain boundary shapes are dominated by irregular and rounded crystal outlines, irrespective of a biotite- or cummingtonite-rich matrix (Figs. 4A-4D), reminiscent of concretionary and colloform textures. Replacement or simultaneous growth textures are not clear. A characteristic feature is that most garnets appear with sphalerite-magnetite encrustrations (Fig. 4A), or with sphalerite-magnetite-filled fractures, that do not continue into the matrix (Figs. 4B-4C). In addition, some garnets enclose the original layering (Fig. 4D). These textures, in combination with the monomineralic layers, suggest that garnet, magnetite and sphalerite were derived from one iron-zinc-bearing siliceous precursor from which magnetite and sphalerite were expelled during crystallization of the garnet.

*Biotite* is present as greenish, fine-grained, anhedral to subhedral crystals with a preferred orientation parallel to the foliation and layering (Figs. 4A, B, D). Grain sizes are generally smaller than 0.7 mm, in most cases between 5 and 60 $\mu$m. The apparent low degree of biotite-biotite and biotite-garnet grain boundary equilibrations (Figs. 4A, B, D) indicates absence of significant recrystallization. The fine-grained nature of biotite, its preferred orientation parallel to foliation and layering, and the low degree of grain boundary equilibration suggest a diagenetic-hydrothermal origin. Biotite also occurs in veins, 'subophitically' intergrown with sulphides. Small orthite inclusions caused brown pleochroitic haloes in the biotite matrix. Minor replacement by chlorite has been observed.

*Cummingtonite* is a common constituent of the garnet-biotite-rich rocks in the NE part of the ore zone. It occurs in layers as fine-grained aggregates and bundles, accompanied by magnetite, minor garnet, biotite, calcite and traces of sphalerite (Fig. 4B). Cummingtonite-cummingtonite and cummingtonite-garnet grain boundaries are irregular, indicating a low degree of grain boundary equilibration, as for biotite. The abundance of cummingtonite decreases and biotite increases in SW direction towards Tandabergsgruvorna. Cummingtonite is absent further SW towards Lake Älvlången (Fig. 1).

*Table 2.* Representative electron microprobe analyses of garnets from the Älvlången-Vikern zinc-lead mineralization (Hellingwerf et al., in prep.).

| | 513GA | | 513GD | | 532GB | | 532GC | | 537AC | | 537CC | |
|---|---|---|---|---|---|---|---|---|---|---|---|---|
| | core | rim | core | rim | core | rim | core | rim | core | rim | core | rim |
| $SiO_2$ | 37.2 | 37.0 | 36.7 | 36.8 | 37.3 | 37.0 | 37.0 | 37.5 | 36.6 | 37.4 | 36.5 | 36.5 |
| $TiO_2$ | – | 0.04 | – | – | – | – | – | – | 0.05 | – | – | 0.04 |
| $Al_2O_3$ | 20.7 | 20.5 | 20.5 | 21.0 | 20.9 | 20.9 | 20.9 | 21.0 | 20.5 | 20.7 | 20.5 | 20.2 |
| FeO | 33.5 | 24.7 | 26.9 | 32.5 | 33.1 | 30.1 | 32.0 | 33.1 | 21.7 | 26.9 | 22.9 | 19.4 |
| MnO | 3.4 | 12.4 | 11.0 | 5.56 | 6.39 | 11.3 | 7.05 | 5.28 | 16.4 | 10.8 | 16.3 | 21.1 |
| MgO | 1.69 | 0.47 | 0.58 | 1.06 | 0.77 | 0.46 | 0.75 | 0.69 | 0.49 | 0.76 | 0.64 | 0.66 |
| CaO | 3.42 | 5.11 | 4.53 | 3.41 | 3.21 | 2.05 | 2.53 | 3.96 | 4.48 | 4.52 | 3.42 | 1.76 |

Samples 513 are from Kopparskallen, 532 from Tandaberg, 537 from Vikersgård (Fig. 1).

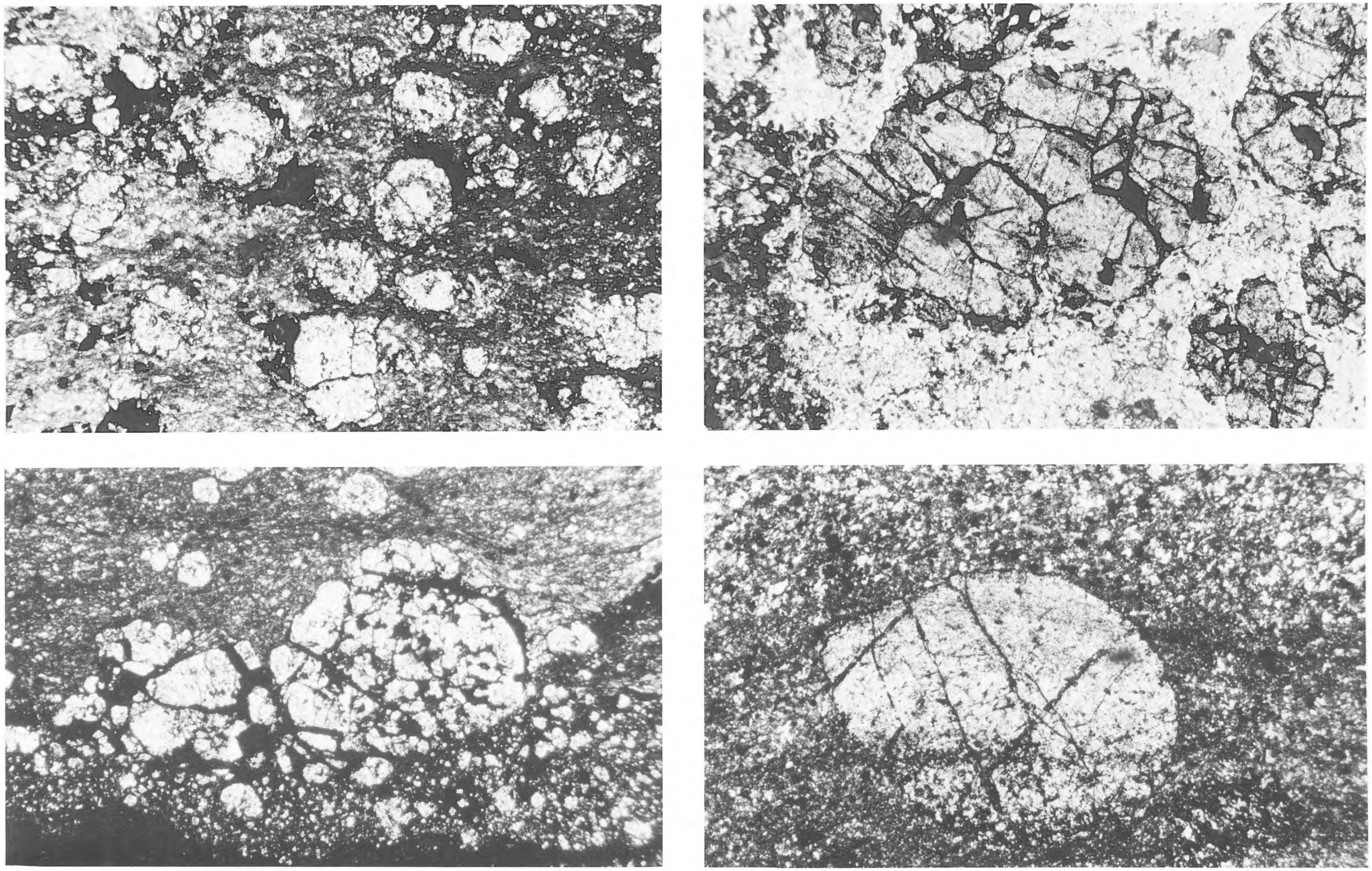

*Fig. 4A*. Microphotograph of zoned garnet porphyroblasts with encrustrations and tiny fractures of sphalerite and magnetite. Note the colloform textures. Plane polarized light. Field of view is 3 × 2 mm; *Fig. 4B*. Microphotograph of garnet porphyroblasts with sphalerite-magnetite-filled fractures, that do not continue into the fine-grained cummingtonite matrix. Note the lack of garnet crystal shapes. Kopparskallen, plane polarized light. Field of view is 3 × 2 mm; *Fig. 4C*. Microphotograph of zoned poikiloblastic garnet aggregates with abundant sphalerite-magnetite-filled fractures that do not continue into the fine-grained biotite matrix. Note the lack of garnet crystal shapes. Tandaberg, plane polarized light. Field of view is 3 × 2 mm; *Fig. 4D*. Microphotograph of oval garnet porphyroblast with enclosed laminations. The lack of garnet crystal shapes is a characteristic feature of the sedimentary-exhalative-diagenetic garnets. W of Älvlången, plane polarized light. Field of view is 3 × 2 mm.

*Sphalerite* is the most prominant ore-mineral and occurs in various ways: 1) as fracture-fillings in and intergrowths with Mn-bearing garnet, 2) as intimate intergrowths with euhedral biotite and cummingtonite ('subophitic' textures), 3) with pyrrhotite in thin sulphide lenses of a few mm long, parallel to the layering in garnet-biotite-rich rocks, and 4) as fine-grained disseminations in biotite-quartz-rich metachert. In veins, sphalerite is also 'subophitically' intergrown with phlogopite/biotite and clinochlore. On the basis of these textures it is concluded that sphalerite crystallized simultaneously with the Ca-Fe-Mn-silicates. Apparently, sphalerite is preferably incorporated in biotite- rather than in cummingtonite-rich layers. Sphalerite concentrations increase from the NE part of the ore zone towards the SW, with a maximum content near Erntorp, and then decreases again further SW across Lake Älvlången (Figs. 1, 11A).

*Galena* occurs 1) as dusty disseminations in fine-grained metachert and garnet-biotite-rich rocks, and 2) as vein-fillings with sphalerite, magnetite, pyrite, quartz, cummingtonite, calcite, or clinochlore, 'subophitically' intergrown with the latter. Galena parallels the behaviour of sphalerite; it increases from the NE part of the ore zone towards the SW, with a maximum content near Erntorp, and then decreases again further SW across Lake Älvlången (Figs. 1, 11B).

*Tourmaline* occurs as blue-green, fine-grained stubs, concentrated in layers up to 5 mm thick, together with biotite, phlogopite and/or epidote (Figs. 3, 5), and in veins cross-cutting the layering. Tourmaline comprises up to 60 vol.% in these layers, referred to as 'tourmalinites' (Nicholson, 1980; Slack, 1982). Tourmalinites occur in marbles, calc-silicate rocks and garnet-biotite-rich rocks. Individual poikiloblasts also occur in the biotite-rich layers of the laminated garnet-biotite-rich samples. Microprobe analyses indicate schorl-rich compositions with minor dravite and uvite components (Hellingwerf et al., in prep.). The distribution of tourmaline partly parallels the behaviour of sphalerite and galena, by increasing in NE-SW direction towards Tandabergsgruvorna, as well as in SW-NE direction towards Erntorp (Fig. 6). Here, whole-rock tourmaline concentrations may be up to 5 vol.% in thin section (Fig. 6).

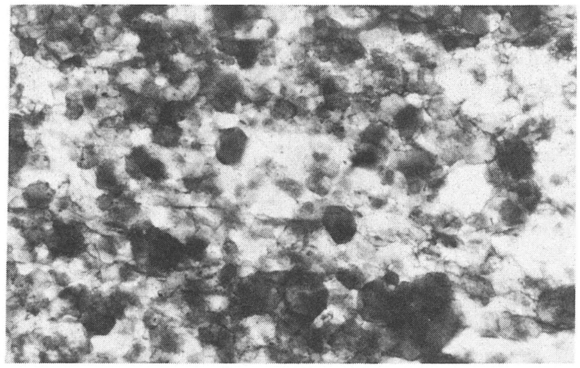

*Fig. 5.* Microphotograph of tourmalinite: fine-grained, euhedral tourmaline stubs (dark grey), concentrated in thin layers with phlogopite and epidote (white). Kopparskallen, plane polarized light. Field of view is 0.8 × 0.5 mm.

*Scapolite* is present as 2–3 mm poikiloblasts in biotite-rich metacherts and garnet-biotite-cummingtonite rocks in the peripheral parts of the ore zone. Detailed petrographic descriptions and a discussion on its hydrothermal-metamorphic origin are presented by Oen & Hellingwerf (1988, this issue).

Accompanying minerals are magnetite, arsenopyrite (occasionally with a core of löllingite), chalcopyrite, pyrite, marcasite, ilmenite, Cl-rich anandite, celsian, grunerite, hastingsite, pargasite, orthite, sphene and apatite.

### *Mineral zonation*

Various mineral zonation patterns have been observed. Cummingtonite-magnetite-rich, sphalerite-galena-poor rocks dominate in the NE part, whereas cummingtonite-magnetite-poor, sphalerite-galena-rich rocks dominate in the central and SW part of the mineralization (Fig. 1). The marble breccias with phlogopite-tourmaline network veins are located below the sphalerite-galena-rich, cummingtonite-magnetite-poor parts of the mineralization (Fig. 1), suggesting that the central and SW parts represent the central part of a submarine basin, in which sulphides were deposited. The NE part then represents the peripheral part of a basin in which manganiferous iron ores and cummingtonite, or its precursor, were deposited. The central and peripheral parts of the mineralization over-

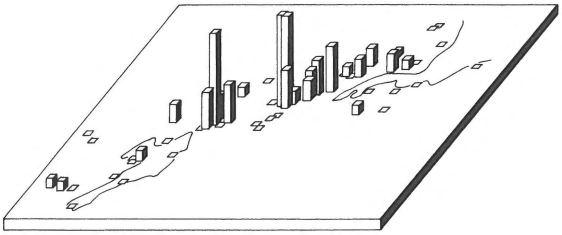

*Fig. 6.* Distribution of tourmaline contents in metavolcanite, marble, metachert and garnet-biotite-cummingtonite-sphalerite-rich rocks. The highest concentrations (5 vol.% whole rock) occur in garnet-biotite-sphalerite-rich rocks at Erntorp and Tandaberg.

lap at Tandabergs- and Västra Viker gruvorna. An equivalent of the cummingtonite-rich rocks in the NE has not been observed SW of Lake Älvlången, leaving the mineralized horizon exposed as an asymmetric configuration.

## Mineralogy of the zinc-lead-hosting marble-metachert sequence

### *Marbles*

The dolomitic to calcitic marbles, hosting the sulphide-rich zone, contain variable amounts of quartz, clinochlore, phlogopite, tremolite, diopside and magnetite. Calc-silicate development along the contacts with metachert layers is the most common alteration type. It resulted in massive diopside skarn with minor tremolite, epidote and sphene. Occasionally small but striking amounts of blue-green, stubby tourmaline occur disseminated throughout the rock. Especially in the footwall marbles in the central part of the basin near Erntorp (Fig. 1), abundant tourmaline is present in phlogopite-rich aggregates. Here, crushed aggregates and broken crystals of tourmaline (2 vol %) occur, giving the rock a cataclastic appearance (Fig. 7). These carbonate-phlogopite-tourmaline-rich rocks show a strong mineralogical resemblence to the marble breccias described in the next section.

### *Footwall marble breccias*

In the marbles, just underlying the sulphide-rich zone, brecciation and network veining has been observed in two lens-shaped zones NE and SW of Lake Älvlången (Figs. 1, 8). On the surface these zones are approximately 100 m thick and 100 to 400 m long, parallel to the zone of mineralization. Presumably the two occurrences are connected with each other under Lake Älvlången, forming one long, NE-SW trending tabular body of breccias, cut across and offset by NS and NW-SE trending faults. The breccias contain angular and subrounded fragments of marble and a purplish-brown rock type resembling rhyolite in a fine-grained,

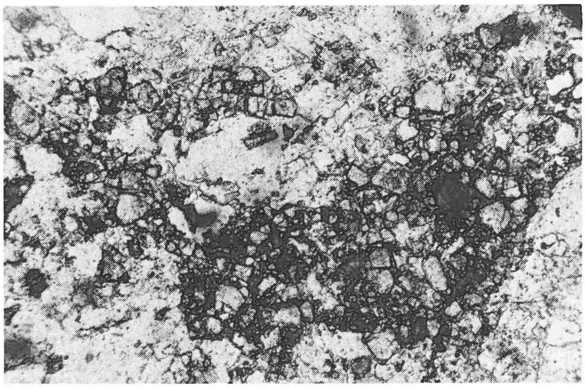

*Fig. 7.* Microphotograph of fragmented tourmaline crystals in phlogopite-bearing marble. The assemblage is similar to that in the NE and SW footwall marble breccias. Erntorp, plane polarized light. Field of view is 3 × 2 mm.

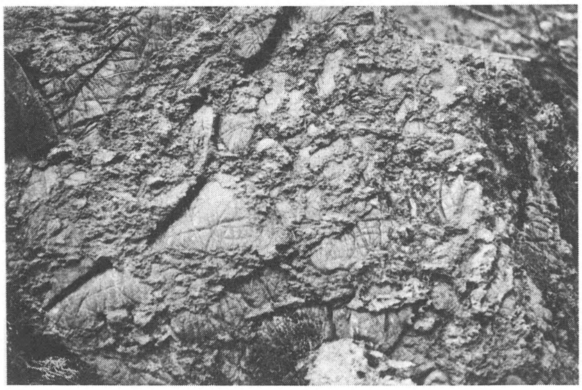

*Fig. 8.* Hydrothermal marble breccia in the footwall of the ore zone. The fractures contain phlogopite, tourmaline and minor tremolite, calcite and magnetite. The SE breccias (W of Älvlången) also contain minor chalcopyrite, pyrrhotite and pyrite. Erntorp. See hammer to the left for scale.

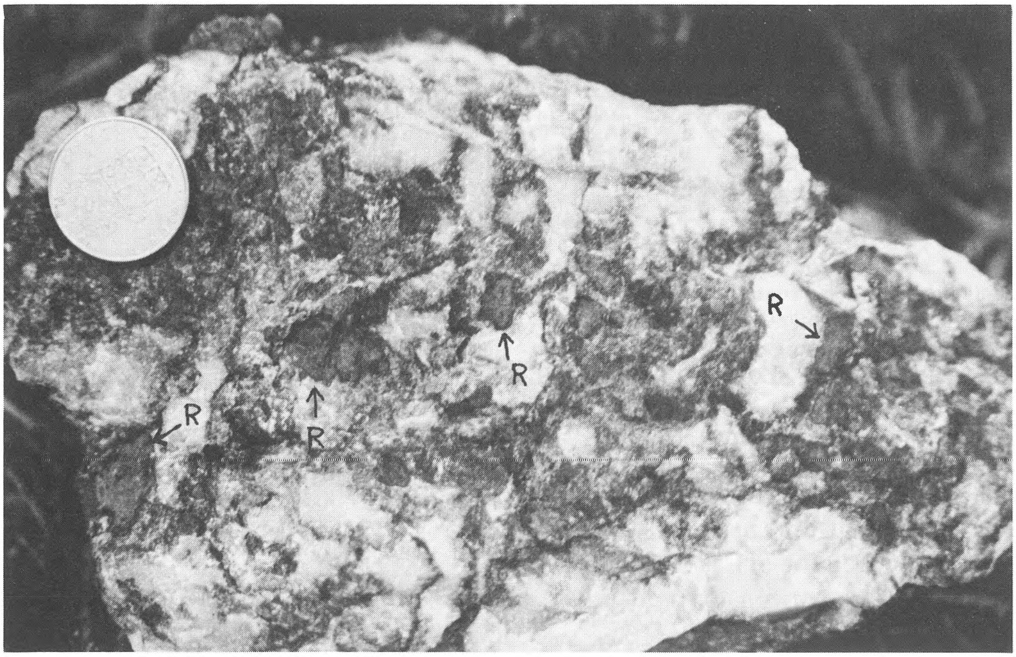


*Fig. 9.* Hydrothermal marble breccia in the footwall of the ore zone. Note the irregular and subrounded marble fragments (white), and the smaller rhyolitic fragments (grey, arrow with R).

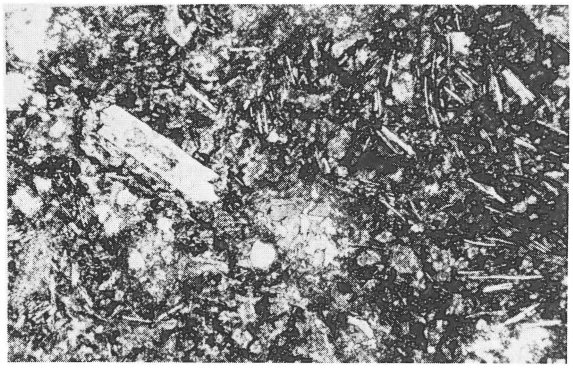

*Fig. 10.* Microphotograph of rhyolitic fragment in footwall marble breccia from Erntorp. Note the pilotaxitic texture of the K-feldspar laths, and the vague amygdules, filled with biotite and sericite. The dark matrix consists of fine-grained biotite, sericite, and hematite replacing magnetite. Plane polarized light. Field of view is 3 × 2 mm.

phlogopite-rich matrix (Figs. 9–10). Tremolite is developed along the rim of the marble fragments and growing into the matrix. Despite this recrystallization and a moderately developed foliation matrix supported textures can still be identified. Besides phlogopite, the matrix consists of tourmaline (up to 5 vol %), minor tremolite, calcite, dolomite, microcline, chlorite and disseminations of magnetite. In addition, the SW breccias contain chalcopyrite, pyrite, pyrrhotite and galena disseminated in the matrix. The significance of chalcopyrite in the breccias and the very low Cu contents in the overlying ore zone is discussed later on.

The rhyolitic fragments are generally much smaller (<5 mm) and much more rounded than the marble fragments. They consist of extremely fine-grained biotite-sericite matrix with abundant opaque dust consisting of hematite and magnetite, and lath-shaped phenocrysts of K-feldspar that show a parallel flow orientation (Fig. 10). Occasionally vesicular textures are prominent, with fine-grained sericite and biotite filling in the amygdules (Fig. 10). Some larger magnetite grains are seen to be replaced by hematite along the rims. The origin of these rhyolitic fragments is yet unclear, though brecciation of a rhyolitic body below the marbles, and upward displacement of the fragments is one possibility. The degree of rounding, greater than that of the marble fragments, suggests that this rock type has been transported from greater depths.

*Metacherts*
The marble-hosted metachert intercalations are presumably products of mixed sedimentary-exhalative and pyroclastic origin. This mixed origin is witnessed by the occurrence of completely aphyric, extremely fine-grained, laminated, sericite-rich rocks of probably chemical-sedimentary origin, that show a gradual transition towards quartz phenocryst-rich rocks with the same micaceous matrix. These rocks occur below and above the mineralized zone, and in the lateral extension of it. Abundant poikilitic and poikiloblastic scapolite may be present, showing signs of a hydrothermal-metamorphic origin. A more detailed description of these fine-grained rocks and the origin of the scapolite is presented by Oen & Hellingwerf (1988, this issue). A study of similar mixed sedimentary-exhalative and pyroclastic rocks, associated with sulphides in the Ljusnarsberg area, 60 km N of the present area, is presented by Parr (1988, this issue).

## Chemical characteristics of the deposit

*General*
The observed zonation of cummingtonite-rich rocks in the peripheral part and cummingtonite-poor rocks in the central part of the mineralized zone is also reflected in the whole rock chemical compositions; the cummingtonite-rich rocks contain significantly more Fe (average: 28 wt%) and Mn, and less A1 and K than the cummingtonite-poor rocks (Table 1). This suggests that cummingtonite is not derived through metamorphism of the garnet-biotite-rich rocks, that occur throughout the mineralized zone, but that 'distal' sedimentary-exhalative fluids entered through the stability field of cummingtonite, or its precursor, under decreasing T and $fS_2$ and increasing $fO_2$ conditions.

In terms of A1, Fe and Mn, the composition of the cummingtonite-rich rocks is strikingly similar to that of the fayalitic iron formation that hosts the Pegmont stratiform Pb-Zn deposit, Queensland (Vaughan & Stanton, 1986). This iron formation, rimmed by garnet-biotite selvages, represents an isochemically metamorphosed basin centre microfacies (Vaughan & Stanton, 1986), whereas the chemically equivalent Älvlången-Vikern rocks represent the basin margin. Possibly this is due to a slightly more oxygenated nature of the Älvlången-Vikern basin (Plimer, writt. comm.).

*Lateral zonations in metachert and garnet-biotite rocks*
The highest *Zn* contents occur at Erntorp (2.8 wt% whole-rock) in the central part of the area, and decrease in NE and SW directions (Fig. 11A). A striking feature is that Zn contents decrease towards Lake Älvlången, though the garnet-biotite-rich host rocks here are similar to those at Erntorp. The distribution patterns of *Pb, Cd* and *Sb* are similar to that of Zn (Figs. 11B, C).

*Fe* contents are highest (37.9 wt%) in the cummingtonite-rich, NE peripheral part of the basin (Table 1). They nearly continuously decrease towards the central part of the basin in the SW (Fig. 11D). The distribution patterns of *Ti, Sc, Cr, Co, Ni, V* and *U* (Fig. 12A) are similar to that of Fe. The patterns of *Mn* and *Ba* are also roughly similar to that of Fe, except for a slight increase, W of Lake Älvlången (Figs. 12B, C). *Zn/Ba* ratios decrease gently from the areas close to the marble breccias towards NE and rather abruptly towards SW (Fig. 12D). Decreasing Zn/Ba ratios away from the feeder zones are common in stratiform deposits (Lydon, 1983).

*Lateral zonations in marble*
*Mn* contents in marble close to the ores show a maximum (1.3 wt%) in the NE and continuously decrease towards the SW (Fig. 13A). This pattern is similar to those of Fe, Mn and Ba in metachert and garnet-biotite rocks (Figs. 11–12). However, marble at higher stratigraphic levels, further away from the ores, shows distinctly lower Mn contents (Fig. 13). *K/Na* ratios are highest in the central part of the area (Fig. 13B), which are attributed to the abundance of phlogopite-rich aggregates in the marble.

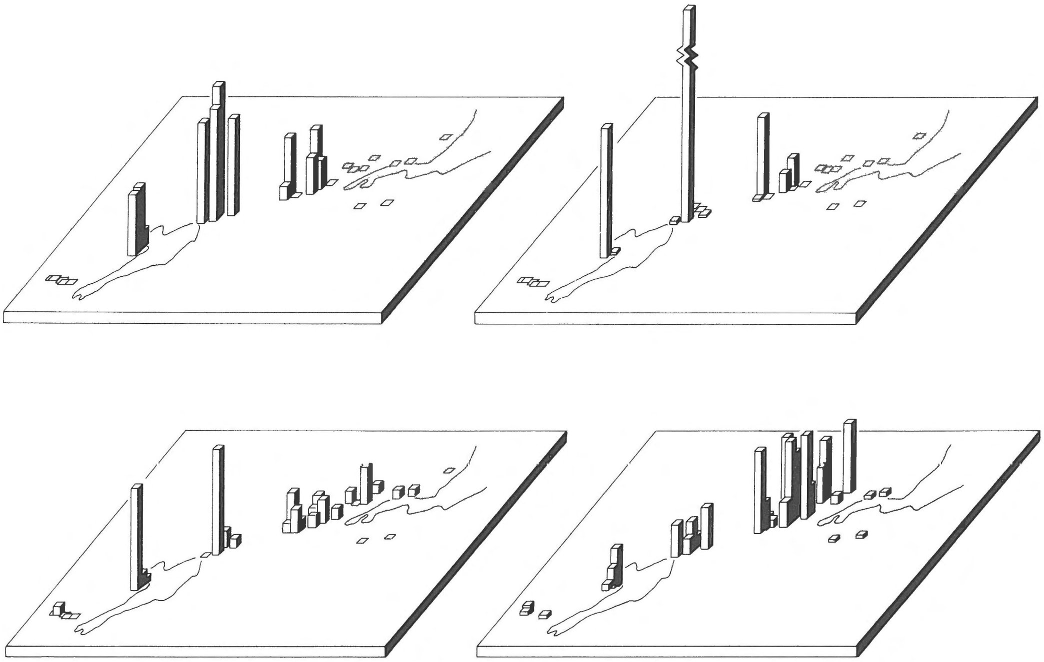

*Fig. 11.* Distribution of metal contents along the metachert-ore horizon; A (upper left) – Zn, maximum content 2.8 wt%; B (upper right) – Pb, maximum contents 6.9 and 1.7 wt%; C (lower left) – Sb, maximum content 98 ppm; D (lower right) – $Fe_2O_3$, maximum content 37.9 wt%. See text for explanation.

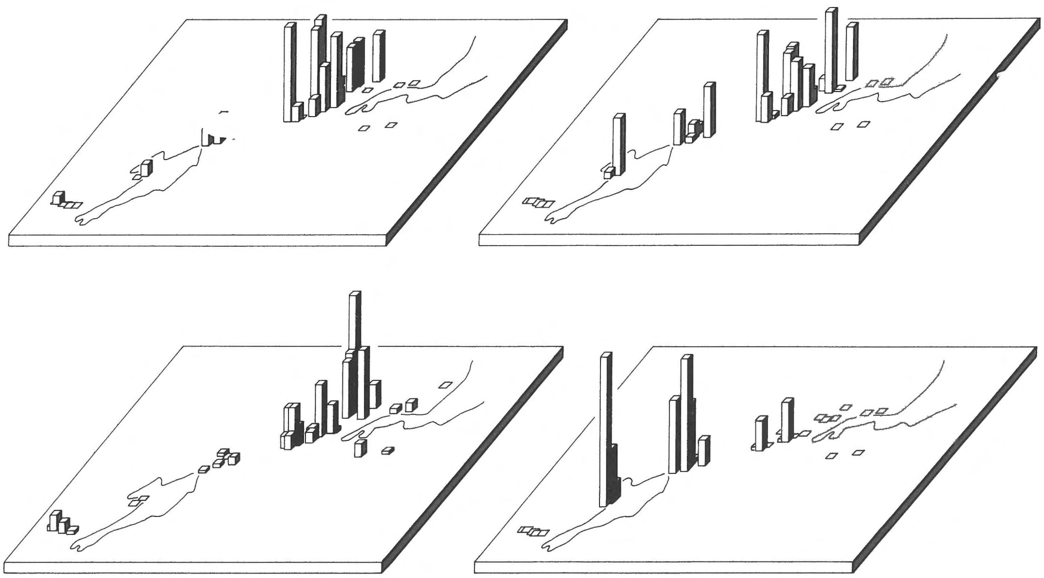

*Fig. 12.* Distribution of metal contents along the metachert-ore horizon; A (upper left) – U, maximum content 200 ppm; B (upper right) – MnO, maximum content 3.6 wt%; C (lower left) – Ba, maximum content 2.3 wt%; D (lower right) – Zn/Ba, maximum value 92.8. See text for explanation.

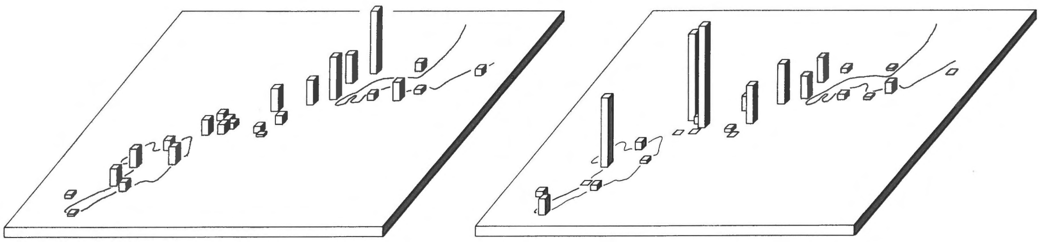

*Fig. 13.* Distribution of metal contents in marble hosting the ore horizon; A (left) – MnO, maximum content 1.3 wt%; B (right) – $K_2O/Na_2O$, maximum value 93.7. See text for explanation.

**Hydrothermal alteration of underlying felsic metavolcanites**

Metavolcanites, underlying the marble-metachert-sulphide zone are felsic pyroclastic rocks with abundant quartz- and feldspar phenocrysts and rock fragments in a fine-grained quartz-feldspar-mica matrix, with minor calcite, epidote, orthite, chlorite and sphene. Various types of alteration are present: weak albitization, various types of potassic alteration, silicification, calc-silicate alteration, and tourmalinization. On average, the whole metavolcanic pile is enriched in potassium, except for one, weakly sodium-enriched sample.

Weak *albitization* (Fig. 14) occurs at the lowest stratigraphic levels, furthest away from the ore zone (Fig. 1). A superficial inspection of the lithogeochemistry of an albitized and a less altered metavolcanite from the same location (Table 1, Fig. 1) suggests that no significant element mobility accompanied albitization. However, the less altered metavolcanite shows some evidence for weak, regional potassic alteration, and may therefore represent a slightly altered composition. Completely fresh rocks have, however, not been found. Still, the enormous volume of altered rock in this area, underlying the ore zone, suggests that part of the ore-forming elements may have been derived from these lower metavolcanites.

*Potassic alteration* is manifested by microclinization, sericitization and biotitization. *Microclinization* (Fig. 15) and *sericitization* are present in stratigraphic levels above those of albitization in the NE part of the area (Fig. 1). From field observations these alteration types seem (semi-) concordant with the layering and foliation. *Biotitization* occurs along fractures and veins resulting in biotite-networks e.g. below the ore zone (Figs. 1, 16). Extreme biotitization occurs 2 km N of Erntorp and 3 km NW of Lake Älvlången. Epidote, chlorite, apatite, and sphene (around ilmenite) accompany this alteration. The biotitized samples seem enriched in Fe, Ti, P, Sc, V, Zn and Pb, relative to the other metavolcanites.

In order to distinguish regionally – from locally potassic altered metavolcanites, the samples are plotted in a $TiO_2$-Zr diagram (Hellingwerf, 1988). Nine samples plot along a straight line, representing unchanged, magmatic $Zr/TiO_2$ values (Fig. 17). These rocks contain microcline, sericite-muscovite and minor biotite in the matrix. They represent regionally altered metavolcanites, that presumably have little or no bearing on the ore-forming processes (Hellingwerf, 1988). Three samples plot away from this magmatic trend due to enrichments in Ti (Fig. 17). These are the biotitized samples, discussed above, representing locally altered rocks that are presumably closely associated with the ore-forming processes. The enrichments of Fe, Ti, P, Sc, V, Zn and Pb in these samples can therefore be explained by precipitation of these elements from supersaturated hydrothermal fluids during transport, before reaching the seafloor.

*Silicification*, occurring 0.5–1 km N of the ore zone, is present as quartz-filled networks, giving the rocks a breccia-like appearance (Fig. 18A). However, the fragments are not rotated, their foliation is plan-parallel, and the veins are aligned in a specific polygonal pattern (Fig. 18B). The relationship between this silicification here, and the

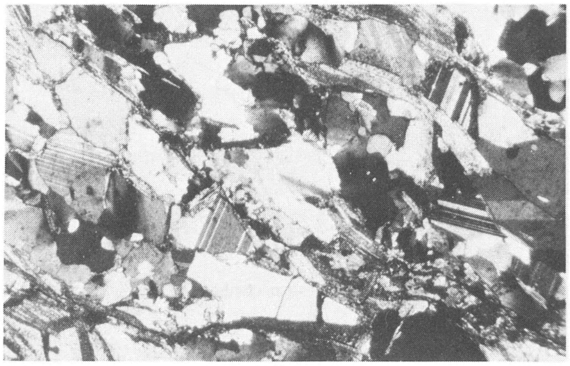

*Fig. 14.* Microphotograph of albitized felsic metavolcanite, 1 km N of Kopparskallen. The foliation is expressed by elongate, undulose quartz grains (white) and a parallel orientation of partly recrystallized muscovite flakes (grey). This type of alteration occurs regionally, and is presumably not directly related to the ore-forming processes. Note the coarse-grained fabric relative to the microclinized equivalent in Fig. 15. Plane polarized light. Field of view is 3 × 2 mm.

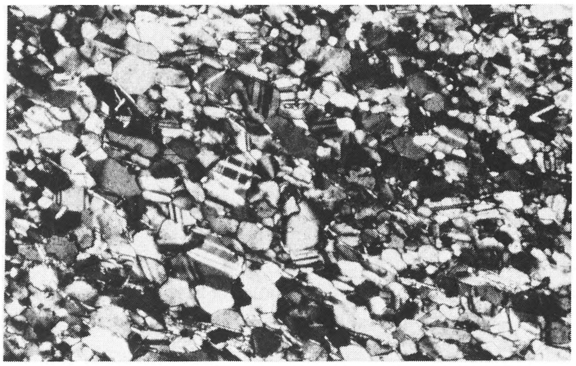

*Fig. 15.* Microphotograph of microclinized felsic metavolcanite, 300 m N of Kopparskallen. This type of alteration occurs regionally, and is presumably not directly related to the ore-forming processes. Note that the fabric is less well recrystallized and finer grained than the albitized equivalent in Fig. 14. Plane polarized light. Field of view is 3 × 2 mm.

phlogopite-tourmaline veining in marble is, however, unclear.

*Calc-silicate alteration* of felsic metavolcanites, defined by the development of amphiboles, pyroxenes and epidote, occurs along fractures crosscutting the layering, and along contacts between metavolcanites and marble below the ore zone. The mode of occurrence, and the extensive rock-fluid interaction, suggests that this alteration type is related to the ore-forming processes.

*Tourmalinization* resulted in the development of poikiloblastic grains up to 1 cm large, but usually smaller, with tiny inclusions of quartz and feldspar. Tourmaline is also intergrown with muscovite, indicating some degree of recrystallization. Locally, aggregates, lenses and boundinaged prisms of tourmaline have been observed, as well as folded quartz-tourmaline veins, suggesting a pre-deformation origin.

## Metamorphism

The stratabound occurrence and extremely well-bedded and laminated character of the Zn-Fe-rich rocks in the Älvlången-Vikern area supports a sedimentary-exhalative origin. Although such an origin is not unique for the base metal, Fe and Mn deposits in Bergslagen (see also Koark, 1962; Berge, 1978; Boström et al., 1979; Bromley-Challenor, 1988, this issue; Damman, 1988, this issue; Carlon & Bleeker, 1988, this issue), very little data has been presented on the possible sedimentary-exhalative origin of the silicate phases. Most of the garnet- and amphibole-rich assemblages, related to mineralization, have been attributed to metamorphism of previously altered rocks (e.g. Wolter & Seifert, 1984; Vivallo, 1985). However, the fact that in the Älvlången-Vikern area Zn-Fe mineralization is restricted to stratabound garnet-biotite-cummingtonite (± scapolite)-rich rocks, also suggests a sedimentary-exhalative origin for the garnet, biotite, cummingtonite and scapolite, or their precursors. According to Oen & Hellingwerf (1988, this issue) there is no need to invoke a regional metamorphic event related to deformation to produce garnet, biotite, cummingtonite and scapolite; all garnet- and cordierite-bearing assemblages in the Älvlången-Vikern area could be attributed to a phase of seafloor, soft rock hydrothermal metamorphism. The data in this study suggest that a metamorphic event, overprinting the sedimentary-exhalative-diagenetic assemblages, is quite unlikely on the basis of 1) the irregular and rounded crystal outlines of garnet, reminiscent of

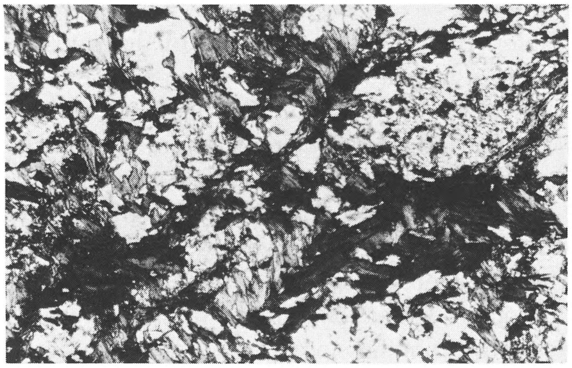

*Fig. 16.* Microphotograph of biotitization affecting felsic metavolcanite, 300 m NW of lake Älvlången. Deformed and recrystallized biotite occurs along fractures and network veins. This type of alteration occurs locally, and is related to the phlogopite veining in the footwall marbles. Plane polarized light. Field of view is 3 × 2 mm.

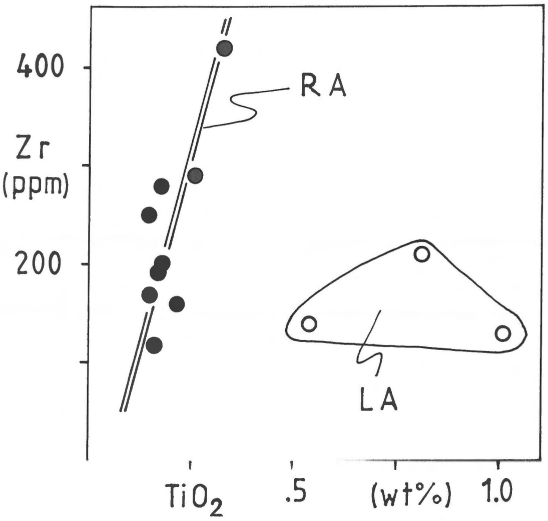


*Fig. 17.* $TiO_2$-Zr diagram to discriminate between regional – and local alteration types. The regionally altered metavolcanites plot along a straight line, representing nearly unaffected (magmatic) Ti-Zr compositions. The locally altered rocks, affected by biotitization, plot away from the magmatic trend, due to enrichment in Ti.

concretionary and colloform textures, 2) the fine-grained nature, and apparent low degree of grain boundary equilibration of biotite and cummingtonite, and 3) the lack of reaction textures. These observations, in combination with the mono-mineralic garnet layers, and the intimate garnet-sphalerite-magnetite intergrowths, suggest that garnet, biotite, cummingtonite, magnetite and sphalerite precipitated as fine-crystalline aggregates or as iron-zinc-manganese-bearing silicate gels onto the seafloor that crystallized under subseafloor hydrothermal-metamorphic conditions (see also Hutchinson, 1983; Stanton, 1986, 1987; Vaughan & Stanton, 1986).

Oen et al. (1986) argued that the Mn-garnets in phyllitic intercalations from the nearby Grythyttan area were formed in a seafloor mud of Ca-Mn-carbonates and cherts under diagenetic-hydrothermal conditions. Also in the silicate facies iron formation at Redstone, Ontario, Mn-garnet and stilpnomelane in low grade metamorphic rocks are suggested to have formed from an exhalative-sedimentary mud (Robinson, 1984). In addition, andradite, pyroxene and amphibole have been found as authigenic products in the Red Sea metal-bearing oozes (Zierenberg & Shanks, 1983). The formation of authigenic garnets in carbonate muds, undergoing hydrothermal seafloor alteration, has been reported by Easton et al. (1977, 1982) to take place at temperatures of 170° C. Such temperatures would be possible under high geothermal gradient conditions, as is suggested to be the case beneath many of the sediment-hosted exhalative zinc-lead deposits (Russell et al., 1981). These observations support the above conclusion that the silicate assemblages in the ore-bearing horizon of the Älvlången-Vikern area could well be products of the sedimentary-exhalative ore-forming processes.

## Reconstructed scenario

The ore zone is envisaged to have formed in a volcano-sedimentary environment just above the boundary of felsic volcanism and incipient carbonate-chert precipitation in a NE-SW trending depression on the seafloor. The depression is bounded on the northern side by a fault zone. Hydrothermal solutions, carrying Si, Al, Zn, Pb, Fe, Mn, Ba, C1, B and traces of Cu, Sb and As, migrated upwards along the fault zone. Boiling of the solutions, a common feature in sedimentary-exhalative pro-

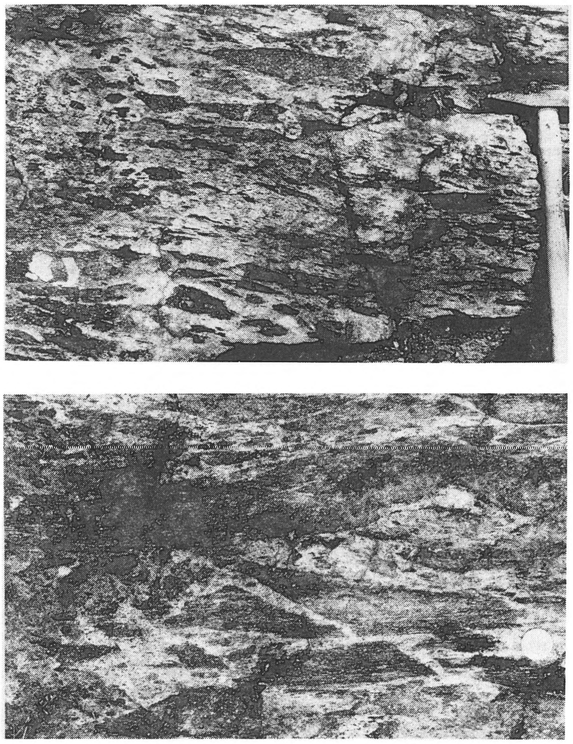

*Fig. 18A.* Silicification affecting felsic metavolcanite along network veins. View perpendicular to the plane of foliation; note the shingle textures of the 'fragments'. *Fig. 18B.* Silicification affecting felsic metavolcanite along network veins. View parallel to the plane of foliation; note the unrotated nature of the 'fragments'.

cesses (Finlow-Bates & Large, 1978), resulted in a build-up of steam, leading to the formation of ore-related breccias. At the lowest stratigraphic levels silicification, biotitization and calc-silicate alteration affected the metavolcanites along networks (Figs. 16, 18–19). Tourmalinization occurred more diffusely. Adiabatic boiling of the solutions and decreasing pressure during their way up lead to a drop in temperature and precipitation of the most insoluble phases, chalcopyrite and pyrrhotite, in the feeder zone (Large, 1977; Finlow-Bates & Stumpfl, 1979). The fact that chalcopyrite has not been observed in the most central breccia, but does occur as a minor phase in the overlying Zn-Pb-B-rich zone, whereas it has been observed in the southwesternmost breccia, away from the central zone (Fig. 19), suggests that water depth was a controlling factor on the solubility of the sulphides (Finlow-Bates, 1980). The bulk of the sulphides remained in solution, together with Si, Al and B, and reached the seafloor. Presumably, precipitation occurred under quiet conditions, considering the finely laminated nature of the deposit. Mineral zoning (sulphides-tourmaline → magnetite-cummingtonite) and chemical zoning (Zn-Pb-B → Fe-Mn-Ba-U) presumably reflect the positioning of the foci of emanation, with continuous precipitation away from these points towards the margins of the basin, where more oxidising conditions prevailed.

The circulation of the hydrothermal fluids is initiated during rifting and driven by a high geothermal gradient beneath the depression. This high geothermal gradient may partially be attributed to a hidden felsic magma plug below the ore zone, as indicated by the rhyolitic fragments in the footwall marble breccias. The presence of tourmaline in metavolcanites below the ore zone, in the footwall hydrothermal marble breccias, and within the ore zone as abundant disseminations and concentrations in layers, indicates that B was an important constituent of the ore-forming system. Its abundance suggests that enough B was at hand not only for precipitating tourmaline, but for transporting metals as well (cf. Bassett, 1980; Plimer, 1983). The origin of the bulk of the metals, S, Cl and B is not quite clear. Firstly, the alteration in the metavolcanites below the ore zone may have involved mobility of ore-forming elements, although most of the alteration types are not typical for sulphide-mineralizing systems (Hellingwerf, 1988). Secondly, a seawater derivation for S and B is possible, but not likely, since most of the volcaniclastic rocks in Bergslagen are water-laid sediments that inevitably have reacted with seawater, and only a very small proportion of these rocks contain tourmaline and sulphides. In addition, only the metavolcanites below the central part of the Älvlången-Vikern deposit contain tourmaline. However, it is to be expected that seawater contributed Cl to the ore-forming fluids. Thirdly, a magmatic origin for the B, Cl and at least part of the metals is possible, considering the high metal, B and Cl contents in active geothermal areas (Haymon & Kastner, 1981;

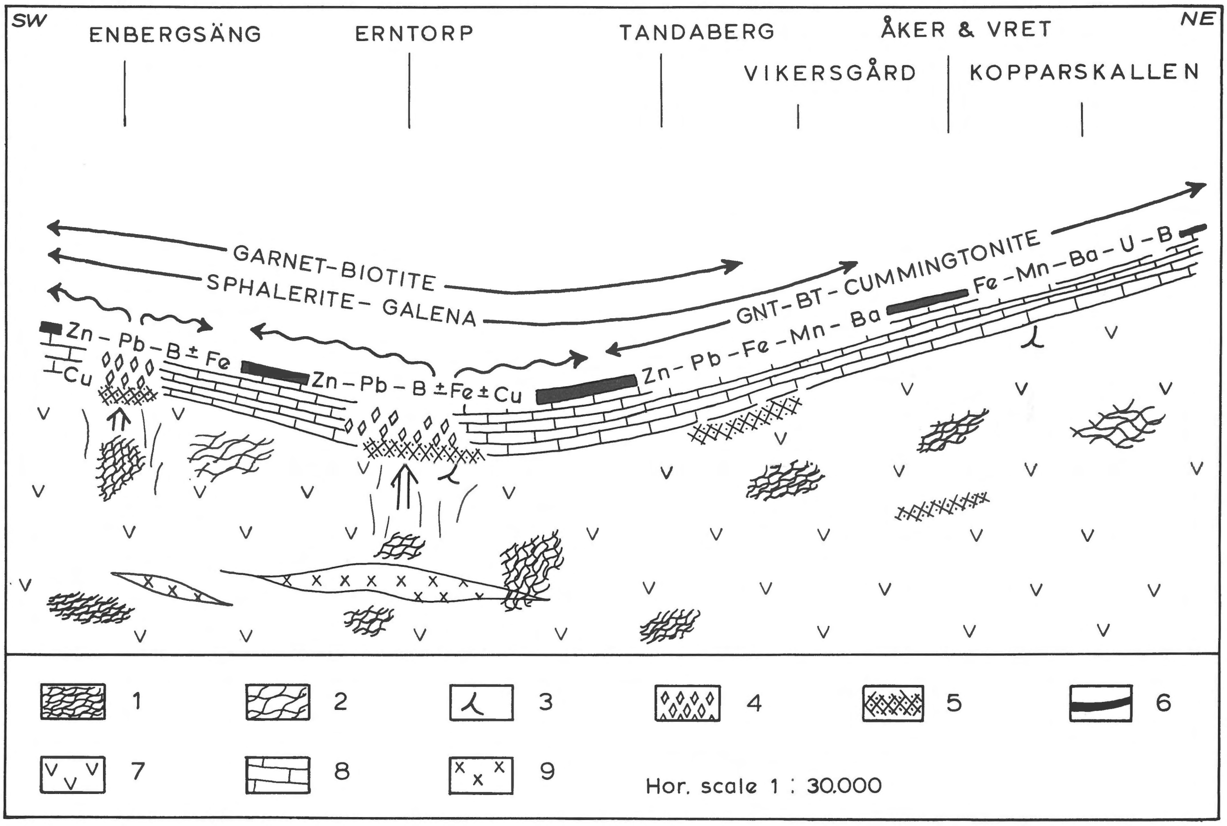


*Fig. 19.* Reconstructed scenario, view perpendicular to the fault plane. 1 – biotitization; 2 – silicification; 3 – quartz-tourmaline veins; 4 – phlogopite-tourmaline alteration in marble breccias; 5 – calc-silicate alteration; 6 – ore zone; 7 – metavolcanite; 8 – marble with metachert and metatuffite intercalations; 9 – metabasite. See text for explanation.

Pottorf & Barnes, 1983; Waring, 1965; Ellis, 1979). The rhyolitic fragments in the footwall marble breccias suggest in any case the presence of a magmatic mass below the ore zone. Therefore, the ore-forming fluid is believed to be of mixed magmatic-seawater derivation.

## Prospection tools

*Tourmaline.* The spatial relationship of tourmaline-phlogopite networks in marble breccias underlying the zinc ores and the stratabound tourmaline-biotite layers within these zinc ores (Figs. 3, 5, 6, 19) indicate a common origin for the zinc mineralization and tourmalinization. In addition, it is evident from microscopic and geochemical considerations that the tourmaline is non-detrital, non-regional metasomatic and non-igneous, leaving a submarine-hydrothermal and/or sedimentary-exhalative, though perhaps somewhat recrystallized, origin. The anomalous occurrence of tourmaline in the vicinity of the highest Zn concentrations is compelling evidence for a genetic association. Therefore tourmaline is expected to act as an appropriate guide mineral in prospecting for zinc deposits. The use of tourmaline as an exploration guide has also been suggested for stratabound sulphide deposits in the North Atlantic Appalachian-Caledonian areas of North America, Scandinavia and the British Isles (Ethier & Campbell, 1977; Slack, 1982; Brown & Ayuso, 1984; Slack et al., 1984).

*Lithogeochemistry.* Increasing K/Na ratios in marbles, and increasing Zn/Ba ratios, and decreasing Fe, Ti, Sc, Co, Ni, V, U, Mn and Ba contents in garnet-biotite-rich rocks towards the central part of the basin are suggested to act as suitable prospection tools for stratiform sulphide mineralizations. The higher concentrations of Mn and Ba in the peripheral part of the Zn/Pb mineralization, and Zn/Ba ratios, decreasing away from the feeder zones, appear to be common features in strata-bound base metal deposits (e.g. Russell, 1974; Gwosdz & Krebs, 1977; Stumpfl, 1979; Lydon, 1983; Finlow-Bates, 1987).

## Conclusions

1) On the basis of petrographic observations it is suggested that garnet, biotite, cummingtonite, magnetite and sphalerite precipitated as fine-crystalline aggregates or as iron-zinc-manganese-bearing silicate gels onto the seafloor, and crystallized in a sub-seafloor hydrothermal-diagenetic environment.
2) Overprinting regional metamorphic conditions, related to deformation, are unlikely to have produced the garnet-biotite-cummingtonite-rich assemblages, considering a) the irregular and rounded crystal outlines of garnet, reminiscent of concretionary and colloform textures, b) the fine-grained nature, and apparent low degree of grain boundary equilibration of biotite and cummingtonite, and c) the lack of reaction textures.
3) Tourmaline, having a wider lateral distribution than the sulphide zone, and occurring in the meta-volcanites below this zone, is suggested to be a guide mineral for other stratiform Zn-Pb mineralizations in Bergslagen.

## Acknowledgements

We are indebted to Prof. Dr. I.S. Oen (University of Amsterdam), Prof. Dr. I.R. Plimer (University of Newcastle, NSW), J.H. Baker (Geologisch Museum Amsterdam), D.J. Robinson (Westmin Resources Ltd, Ont.) and B. Levi (University of Stockholm) for reading and improving the manuscript. We are also grateful to the State Mining Property Commission, Stockholm, Sweden, for permission to publish the data from the on-going Älvlången-Vikern project. We also thank Elcira Lilljequist (Uppsala) for preparation of the polished thin sections, F. Kievits (Geologisch Instituut, Amsterdam) for the drawings, and J. Wiersma (Geologisch Instituut, Amsterdam) for the photographs.

## References

Baker, J.H. 1985. The petrology and geochemistry of 1.8–1.9 Ga granitic magmatism and related sub-seafloor hydrothermal alteration and ore-forming processes, W. Bergslagen, Sweden – GUA Papers of Geology, Ser. 1, 21: 204 pp

Basset, R.L. 1980. A critical evaluation of the thermodynamic data for boron ions, ion pairs, complexes, and polyanions in aqueous solution at 298.15 K and 1 bar – Geochim. Cosmochim. Acta, 44: 1151–1160

Berge, J.W. 1978. A re-examination of the association of magnesium and massive sulfide ore – Geol. För. Förh., 100: 155–170

Boström, K., Rydell, H. & Joensuu, O. 1979. Långban – an exhalative sedimentary deposit? – Econ. Geol., 74: 1002–1011

Bromley-Challenor, M. 1988. The Falun Supracrustal Belt. In: Baker, J.H. & Hellingwerf, R.H. (eds): The Bergslagen Province, Central Sweden – Structure, stratigraphy and ore-forming processes. I.G.C.P. project 247 – Geol. Mijnbouw, 67: 239–253 (this issue)

Brown, C.E. & Ayuso, R.A. 1984. Significance of tourmaline-rich rocks in the Grenville complex of St. Lawrence County, New York – U.S. Geol. Surv. Bull., 1626-C

Carlon, C. & Bleeker, W. 1988. The geology and structural setting of copper, arsenic, cobalt, bismuth, gold mineralization at Håkansboda, Bergslagen, central Sweden. In: Baker, J.H. & Hellingwerf, R.H. (eds): The Bergslagen Province, Central Sweden – Structure, stratigraphy and ore-forming processes. I.G.C.P. project 247 – Geol. Mijnbouw, 67: 279–292 (this issue)

Damman, A.H. 1988. Exhalative-sedimentary manganiferous iron ores from the Gåsborn area, W. Bergslagen, C. Sweden. In: Baker, J.H. & Hellingwerf, R.H. (eds): The Bergslagen Province, Central Sweden – Structure, stratigraphy and ore-forming processes. I.G.C.P. project 247 – Geol. Mijnbouw, 67: 433–442 (this issue)

Easton, A.J., Hamilton, D., Kempe, D.R.C. & Sheppard, S.M.F. 1977. Low temperature metasomatic garnets in marine sediments – Phil. Trans. Royal Soc. London, Ser. A 286: 253–271

Easton, A.J., Joslin, I.E., Kempe, D.R.C. & Hancock, J.M. 1982. Metasomatic alteration of pelagic ooze on spreading ocean ridges – Marine Geol., 48: M1-M6

Ellis, A.J. 1979. Explored geothermal systems. In: H.L. Barnes (eds.): Geochemistry of hydrothermal ore deposits – Wiley & Sons, (New York) 2nd ed. 632–683

Ethier, V.G. & Campbell, F.A. 1977. Tourmaline concentrations in Proterozoic sediments of the southern Cordillera of Canada and their economic significance – Can. J. Earth Sci., 14: 2348–2363

Finlow-Bates, T. 1980. The chemical and physical controls on the genesis of submarine exhalative orebodies and their implications for formulating exploration concepts. A review – Geol. Jb., D40: 131–168

Finlow-Bates, T. 1987. The possible significance of uncommon barium-rich mineral assemblages in sediment-hosted lead-zinc deposits – Geol. Mijnbouw, 66: 65–66

Finlow-Bates, T. & Large, D. 1978. Water depth as a major control on the formation of submarine exhalative ore deposits – Geol. Jb., D30: 27–39

Finlow-Bates, T. & Stumpfl, E.F. 1979. The copper and lead-zinc-silver orebodies of Mt. Isa Mine, Queensland: products of one hydrothermal system – Ann. Soc. Geol. Belgique, T. 102: 497–517

Geijer, P. & Magnusson, N.H. 1944. De mellansvenska järnmalmernas geologi – Sver. Geol. Unders., Ser. Ca 35

Gwosdz, W. & Krebs, W. 1977. Manganese halo surrounding Meggen ore deposit, Germany – Trans. Inst. Min. Metall., 86: B73–B77

Haymon, R.M. & Kastner, M. 1981. Hot springs deposits on the East Pacific Rise at 21° N: Preliminary description of mineralogy and genesis – Earth Planet. Sci. Lett., 53: 363–381

Hellingwerf, R.H. 1986. Contributions to the geology and ore genesis of Western Bergslagen, Sweden: Ph.D. thesis GUA Pap. Geol. Ser. 1, 25: 260 pp

Hellingwerf, R.H. 1988 Regional and local potassic alterations in western Bergslagen and their relation to sulphide mineralization – Proc. 7th IAGOD Symp., Luleå

Hellingwerf, R.H. & Baker, J.H. 1985. Wall-rock alteration and tungsten and molybdenum mineralizations associated with older granites in western Bergslagen, Sweden – Econ. Geol., 80: 479–487

Hellingwerf, R.H. & Oen I.S. 1986. Some geochemical aspects of altered and least altered metabasic rocks in the Saxå area, Bergslagen, Sweden – N. Jahrbuch Miner., Monatsh 2: 65–81

Helmers, H. 1984. Stages of granite intrusion and regional metamorphism in the Proterozoic rocks of Western Bergslagen, C. Sweden, as exemplified in the Grängen area – N. Jahrb. Miner., 150: 307–324

Hietanen, A. 1975. Generation of potassium-poor magmas in the Nortern Sierra Nevada and the Svecofennian of Finland – J. Res. U.S. Geol. Surv., 3: 631–645

Hutchinson, R.W. 1983. Hydrothermal concepts: the old and the new – Econ. Geol., 78: 1734–1741

Koark, H.J. 1962. Zur Alterstellung und Entstehung der Sulfiderze vom Typus Falun – Geol. Rundsch., 52: 123–145

Large, R.R. 1977. Chemical evolution and zonation of massive sulfide deposits in volcanic terrains – Econ. Geol., 72: 549–572

Loberg, B.E.H. 1980. A Proterozoic subduction zone in southern Sweden – Earth Planet. Sci. Lett., 46: 287–294

Löfgren, C. 1979. Do leptites represent Precambrian island arc rocks? – Lithos, 12: 159–165

Lydon, J.W. 1983. Chemical parameters controlling the origin and deposition of sediment-hosted stratiform lead-zinc deposits. In: Sangster, D.F. (ed.): Sediment-hosted Stratiform Lead-zinc Deposits. Short course Handbook – Min. Assoc. Can., 8: 175–250

Magnusson, N.H. 1950. Zinc and lead deposits of central Sweden: Int. Geol. Congr., Rep. 18th session, VII, London: 371–379

Nicholson, P.M. 1980. The geology and economic significance of the Golden Dyke dome, Northern Territory. In: Ferguson, J. & Goleby, A.B. (eds): Uranium in the Pime Creek geosyncline: Vienna – Int. Atomic Energy Agency: 319–334

Oen, I.S. 1987. Rift-related igneous activity and metallogenesis in SW Bergslagen, Sweden – Precambr. Res. 35: 367–382

Oen, I.S., Helmers, H., Verschure, R.H. & Wiklander, U. 1982. Ore deposition in a Proterozoic rift zone environment: A tentative model for the Filipstad-Grythyttan-Hjulsjö region, Bergslagen, Sweden – Geol. Rundsch., 71: 182–194

Oen, I.S., De Maesschalck, A.A. & Lustenhouwer, W.J. 1986. Mid-Proterozoic exhalative-sedimentary Mn-skarns containing possible microbial fossils, Grythyttan, Bergslagen, Sweden – Econ. Geol., 81: 1533–1543

Oen, I.S. & Hellingwerf, R.H. 1988. Textural evidence for seafloor, soft rock hydrothermal metamorphism in a garnet-scapolite-bearing metatuffite-exhalite-skarn-sphalerite ore sequence, Nora, Bergslagen, Sweden. In: Baker, J.H. & Hellingwerf, R.H. (eds): The Bergslagen Province, Central Sweden – Structure, stratigraphy and ore-forming processes. I.G.C.P. project 247 – Geol. Mijnbouw, 67: 333–348 (this issue)

Parr, J. 1988. The metasediments associated with strata-bound base metal mineralization, Ljusnarsberg district, central Sweden. In: Baker, J.H. & Hellingwerf, R.H. (eds): The Bergslagen Province, Central Sweden – Structure, stratigraphy and ore-forming processes. I.G.C.P. project 247 – Geol. Mijnbouw, 67: 189–202 (this issue)

Plimer, I.R. 1979. Sulphide rock zonation and hydrothermal alteration at Broken Hill, Australia – Trans. Instn. Min. Metall. (sect. B: Appl. Earth Sci.), 88: B161–189

Plimer, I.R. 1983. The association of tourmaline-bearing rocks with mineralization at Broken Hill, N.S.W. – Aust. Instn. Min. Metall. Ann. Conf., Broken Hill 1983: 157–179

Plimer, I.R. 1986. Sediment-hosted exhalative Pb-Zn deposits – products of contrasting ensialic rifting – Trans. Geol. Soc. S. Afr., 89: 57–73

Pottorf, R.J. & Barnes, H.L. 1983. Mineralogy, geochemistry, and ore genesis of hydrothermal sediments from the Atlantis II Deep, Red Sea – Econ. Geol. Mon., 5: 198–223

Robinson, D.J. 1984. Silicate facies iron-formation and strata-bound alteration: tuffaceous exhalites derived by mixing – Evidence from Mn garnet-stilpnomelane rocks at Redstone, Timmins, Ontario – Econ. Geol., 79: 1796–1817

Russell, M.J. 1974. Manganese halo surrounding the Tynagh ore deposit. Ireland: a preliminary note – Trans. Instn. Mining Metall., 83: B65–B66

Russell, M.J., Solomon, M. & Walshe, J.L. 1981. The genesis of sediment-hosted, exhalative zinc + lead deposits – Mineral. Deposita, 16: 113–127

Sangster, D.F. 1976. Carbonate-hosted lead-zinc deposits. In: K.H. Wolf (ed.): Handbook of strata-bound and stratiform ore deposits, 6 – Elsevier Sci. Publ. Company (Amsterdam)

Sangster, D.F. 1986. Classification, distribution and grade-tonnage summaries of Canadian lead-zinc deposits – Geol. Surv. Can. Economic Geology Rep., 37: 18 pp

Sangster, D.F. & Scott, S.D. 1976. Precambrian, strata-bound, massive Cu-Zn-Pb sulfide ores of North America. In: K.H. Wolf (ed.): Handbook of strata-bound and stratiform ore deposits, 6 – Elsevier Sci. Publ. Company, (Amsterdam): 129–222

Santesson, B. 1889. Beskrivning till karta öfver berggrunden inom norra delarna av Örebro län II. Geognostiska kartor och beskrifningar öfver de viktigare grufvefälten – Sver. Geol. Unders., Ser. Bb 4

Sawkins, F.J. 1986. The recognition of palaeorifting in mid- to late-Proterozoic terranes: implications for the exploration geologist – Trans. Geol. Soc. S. Afr., 89: 223–232

Slack, J.F. 1982. Tourmaline in Appalachian-Caledonian massive sulphide deposits and its exploration significance – Inst. Min. Metall. Trans. 91, Sec. B: B81–B89

Slack, J.F., Herriman, N., Barnes, R.G. & Plimer, I.R. 1984. Stratiform tourmalinites in metamorphic terranes and their geologic significance – Geology, 12: 713–716

Stanton, R.L. 1986. Stratiform ores and geological processes – Instn. Min. Metall. Trans. (Sect. B (Appl. Earth Sci.), 95: B165–178

Stanton, R.L. 1987. Constitutional features, and some exploration implications, of three zinc-bearing stratiform skarns of eastern Australia – Instn. Min. Metall. Trans. Sect. B (Appl. Earth Sci.), 96: B37–57

Stumpfl, E.F. 1979. Manganese haloes surrounding metamorphic stratabound base metal deposits – Miner. Deposita, 14: 207–217

Van der Velden, W., Baker, J., De Maesschalck, S. & Van Meerten, T. 1982. Bimodal early Proterozoic volcanism in the Grythytte field and associated volcano-plutonic complexes, Bergslagen, Central Sweden – Geol. Rundsch., 71: 171–181

Vaughan, J.P. & Stanton, R.L. 1986. Sedimentary and metamorphic factors in the development of the Pegmont stratiform Pb-Zn deposit, Queensland, Australia – Instn. Min. Metall. Trans. Sect. B (Appl. Earth Sci.), 95: B94–121

Vivallo, W. 1985. The origin of the early Proterozoic supracrustal rocks in the Garpenberg district, south central Sweden – Geol. För. Förh., 106: 131–149

Vivallo, W. & Rickard, D. 1984. Early Proterozoic ensialic spreading-subsidence: evidence from the Garpenberg enclave, central Sweden – Precambr. Res., 26: 203–221

Waring, G.A. 1965. Thermal springs of the United States and other countries of the world – a summary – US Geol. Surv. Prof. Pap., 492

Welin, E., Wiklander, U. & Kähr, A.M. 1980. A radiometric study of a quartz-porphyritic K-rhyolite at Hällefors, Örebro, county, Sweden – Geol. För. Förh., 102: 269–272

Wolter, H.U. & Seifert, F. 1984. Mineralogy and genesis of cordierite-anthophyllite rocks from the sulfide deposit of Falun, Sweden – Lithos, 17: 147–152

Zierenberg, R.A. & Shanks, W.C. 1983. Mineralogy and geochemistry of epigenetic features in metalliferous sediment, Atlantis II Deep, Red Sea – Econ. Geol., 78: 57–72